Relation Between Correction Masses and Bearing Forces in a Rigid Rotor

Oh Sung Jun*

(*Received August 27, 1998*)

Bearing forces on a rigid rotor are mainly characterized by unbalance distribution. The forces can be divided into two arbitrary planes along a rotor shaft since any unbalance in the rigid rotor is able to be expressed on two planes. The correction mass quantities on two arbitrary planes are analytically found in terms of the bearing force measurements from the basic concept of three-dimensional rigid body dynamics. The quantities are expressed in terms of the geometry of rotor - the distance between two bearings and the positions of two planes from the bearings - and the bearing forces : amplitudes of the alternating component of forces and angular positions of their peak values. The validity of the proposed method is proved using a simulation example.

Key Words: Rigid Rotor, Correction Mass, Bearing Force, Balancing, Complex Variable

1. Introduction

Unbalance in a rotating body produces an undesirable centrifugal force. The force makes the shaft bend elastically and imposes an excessive force on the bearings which can deteriorate the functions of the rotor and/or eventually decrease the life of the machine. Balancing process on the rotor, therefore, is a necessity for its safe and normal operation. For a rigid rotor, where the flexibility of rotor shaft is negligible, the centrifugal force due to unbalance is directly transmitted to the bearings. Thus the responses (forces or displacements) at the bearings are measured in rotor balancing(ISO 1925, 1981; Everett, 1987; Darlow, 1987; 1989).

The general balancing procedure is composed of attaching the trial mass, running the rotor, measuring the corresponding response and calculating the unbalance. Since only the relative changes of the response by trial mass attachment are measured in the balancing work, there is no severe difficulty in the measurement.

Unbalance in a rigid rotor can be divided into unbalanced masses on the two arbitrary planes perpendicular to the rotating axis. On the other hand, the bearing forces produced by the centrifugal force due to the unbalance are determined by the axial and circumferential positions of the unbalance, its magnitude and the rotating speed of rotor. Thus the (time-dependent) bearing forces can be expressed on the two arbitrary planes along the shaft axis.

Balancing without trial runs has been carried out on hard bearing balancing machine makers and by researchers. (Kwon et al., 1995) They treated the rotor to be balanced as a dummy system and used the relation between input and output on the viewpoint of measurement.

In this study, the relations between rotor skewness and bearing forces, between correction quantities on the balancing planes and bearing forces, and the extraction method of the parameters for calculating the correction quantities through measurements are rigorously derived. A simulation example is used for proving the method.

* School of Mechanical and Industrial Engineering, Jeonju University, Hyoja, Wansan, Jeonju 560-759, Korea.

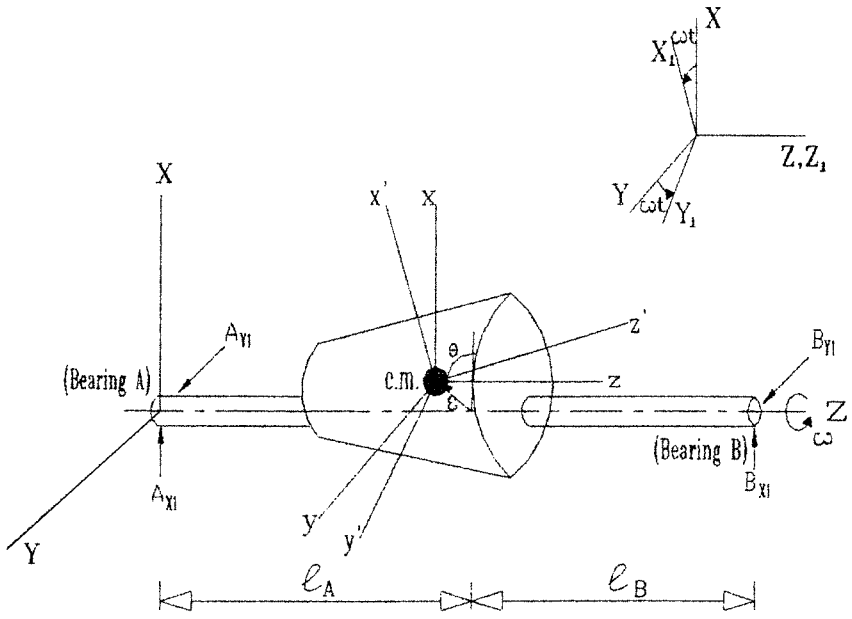

Fig. 1 General rigid rotor having offset of mass center and tilted principal axes.

2. Bearing Force Characteristics of a General Rigid Rotor

2.1 Model

A general rigid rotor model mounted on radially rigid bearings is considered. In Fig. 1, $X-Y-Z$ and $X_1-Y_1-Z_1$ indicate the stationary and rotating coordinates, respectively; the center of mass is located at a distance of ε from the axis of rotation with an angle θ, ω is the constant rotational speed, A_{X_1}, A_{Y_1}, B_{X_1} and B_{Y_1} are the bearing forces at bearings A and B expressed with respect to the rotating coordinates; l_A and l_B are the lengths from the center of mass to the bearings A and B, respectively; and $x-y-z$ and $x'-y'-z'$ having the origins at the center of mass, are rotating coordinates parallel to $X_1-Y_1-Z_1$ and principal axes of the rotor, respectively.

2.2 Motion and moment equations

The force equilibrium equations in the X_1 and Y_1 directions can be expressed as:

$$\sum F_{X_1} = -m\varepsilon\omega^2\cos\theta \tag{1}$$

$$\sum F_{Y_1} = -m\varepsilon\omega^2\sin\theta \tag{2}$$

The Euler equation of three dimensional rigid-body motion is

$$\sum \overline{M}_A = (\overline{H}_A)_{X_1Y_1Z_1} + \overline{\Omega}\times\overline{H}_A \tag{3}$$

where $(\overline{H}_A)_{X_1Y_1Z_1}$ is the time rate of change of angular momentum ($\overline{H}_A$ measured with respect to the $X_1-Y_1-Z_1$ reference). Since this model rotates at a constant speed $\Omega_{Z_1}=\omega$ ($\Omega_{X_1}=\Omega_{Y_1}=0$ and $\Omega_{X_1}=\Omega_{Y_1}=\Omega_{Z_1}=0$), the Eq. (3) yields two equations:

$$\sum M_{X_1} = I_{Y_1Z_1}\omega^2 \tag{4}$$

$$\sum M_{Y_1} = -I_{X_1Z_1}\omega^2 \tag{5}$$

2.3 Bearing forces

By introducing the bearing reaction and gravitational forces and the moments due to the forces into Eqs. (1) to (5), the following equations are obtained:

$$A_{X_1} + B_{X_1} - mg\cos\omega t = -m\varepsilon\omega^2\cos\theta \tag{6}$$

$$A_{Y_1} + B_{Y_1} + mg\sin\omega t = -m\varepsilon\omega^2\sin\theta \tag{7}$$

$$-(l_A+l_B)B_{Y_1} - l_A mg\sin\omega t = I_{Y_1Z_1}\omega^2 \tag{8}$$

$$(l_A+l_B)B_{X_1} - l_A mg\cos\omega t = -I_{X_1Z_1}\omega^2 \tag{9}$$

Using complex variables

$$\overline{A}_1 = A_{X_1} + jA_{Y_1} \tag{10}$$

$$\overline{B}_1 = B_{X_1} + jB_{Y_1} \tag{11}$$

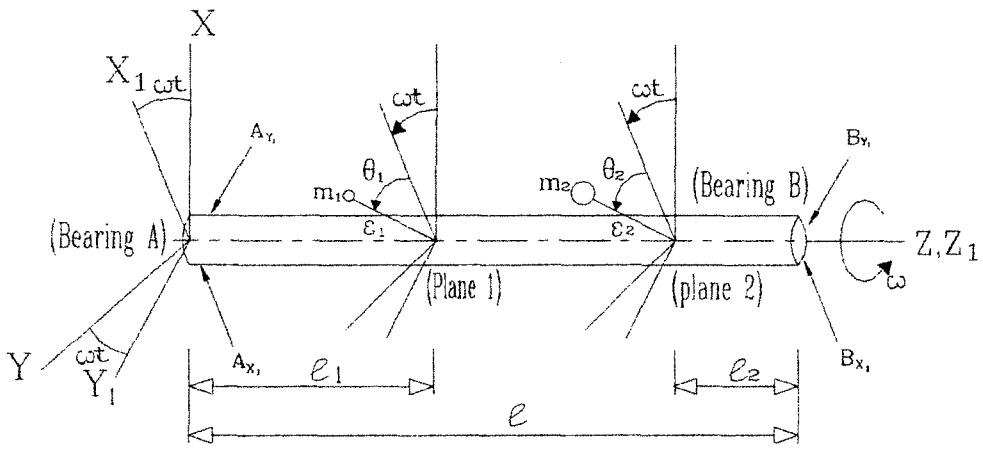

Fig. 2 Balancing rotor model.

Eqs. (6) to (9) yield two equations:

$$\overline{A}_1+\overline{B}_1=mge^{-j\omega t}-m\varepsilon\omega^2e^{j\theta} \quad (12)$$

$$(l_A+l_B)\overline{B}_1=mgl_Ae^{-j\omega t}-(I_{X_1Z_1}+jI_{Y_1Z_1})\omega^2 \quad (13)$$

Equation (13) is replaced by

$$(l_A+l_B)\overline{B}_1=mgl_Ae^{-j\omega t}-ml_A\omega^2\varepsilon e^{j\theta}-(I_{xz}+jI_{yz})\omega^2 \quad (14)$$

since the parallel-axis theorem yields

$$I_{X_1Z_1}=I_{xz}+ml_A\varepsilon\cos\theta$$

$$I_{Y_1Z_1}=I_{yz}+ml_A\varepsilon\sin\theta$$

Solving for $\overline{A}_1$ and $\overline{B}_1$ from Eqs. (12) and (14), we have

$$\overline{A}_1=\frac{1}{l_A+l_B}(mgl_Be^{-j\omega t}-ml_B\omega^2\varepsilon e^{j\theta}+\omega^2(I_{xz}+jI_{yz}) \quad (15)$$

$$\overline{B}_1=\frac{1}{l_A+l_B}(mgl_Ae^{-j\omega t}-ml_A\omega^2\varepsilon e^{j\theta}-\omega^2(I_{xz}+jI_{yz}) \quad (16)$$

The bearing reaction forces expressed on the rotating coordinates have time-dependent terms due to the gravity and time-independent terms due to the rotor skewness composed of ε, θ, I_{xz} and I_{yz}. The forces $\overline{A}_1$ and $\overline{B}_1$ in Eqs. (15) and (16) are actually the reaction from the bearing.

The bearing forces $\overline{A}_1$ and $\overline{B}_1$ due to the rotor skewness used in the following part of this paper have the opposite direction to that of $\overline{A}_1$ and $\overline{B}_1$ in Eqs. (15) and (16).

3. Relation between Bearing Force Measurements and Balancing Plane Quantities

3.1 Modelling

Balancing is a process whereby the offset of the mass center is eliminated and a tilted principal axis of rotation is aligned. In the case of this rigid rotor-bearing system, the offset of mass center and the tilting of the principal axis can be transformed into a dynamically equivalent system by lumping the mass into two planes perpendicular to the rotating axis. Therefore, when we convert the offset and skewness of the rotor by the lumped masses on two planes and apply the corresponding counter weights on the planes, the unbalance can be eliminated dynamically. This indicates two-plane balancing of a rigid rotor.

Figure 2 shows two lumped masses m_1, m_2 on the planes 1 and 2, where ε_1, ε_2 and θ_1, θ_2 indicate the eccentricities and orientations of the masses, respectively. The planes 1 and 2 are located at the distances of l_1 and l_2 inside from the bearings A and B, respectively.

3.2 Equations of motion

For the lumped-mass system of Fig. 2, the equations of force equilibrium on the rotating coordinates are expressed as follows:

$$A_{X1}+B_{X1}-(m_1+m_2)g\cos\omega t+m_1\varepsilon_1\omega^2\cos\theta_1+m_2\varepsilon_2\omega^2\cos\theta_2=0 \quad (17)$$

$$A_{Y1}+B_{Y1}+(m_1+m_2)g\sin\omega t+m_1\varepsilon_1\omega^2\sin\theta_1+m_2\varepsilon_2\omega^2\sin\theta_2=0 \quad (18)$$

The moment equilibrium equations on the rotating coordinates with respect to the bearing position A are written as:

$$-l_1m_1\varepsilon_1\omega^2\sin\theta_1-(l-l_2)m_2\varepsilon_2\omega^2\sin\theta_2-l_1B_{Y1}-l_1m_1g\sin\omega t-(l-l_2)m_2g\sin\omega t=0 \quad (19)$$

$$l_1m_1\varepsilon_1\omega^2\cos\theta_1+(l-l_2)m_2\varepsilon_2\omega^2\cos\theta_2+l_1B_{X1}-l_1m_1g\cos\omega t-(l-l_2)m_2g\cos\omega t=0 \quad (20)$$

3.3 Derivation of correction quantities in terms of bearing forces

As can be seen in Eqs. (17) to (20), the quantities m_1, m_2, $m_1\varepsilon_1$, $m_2\varepsilon_2$, θ_1 and θ_2 are so entangled that it is extremely complicated to solve them explicitly as functions of the bearing forces A_{X1}, A_{Y1}, B_{X1} and B_{Y1}. However, the equations can be simplified by introducing the complex numbers. By summing Eq. (17) and Eq. (18) multiplied by the imaginary number j, the following equation is obtained:

$$(A_{X1}+jA_{Y1})+(B_{X1}+jB_{Y1})-(m_1+m_2)ge^{-j\omega t}+m_1\varepsilon_1\omega^2e^{j\theta_1}+m_2\varepsilon_2\omega^2e^{j\theta_2}=0 \quad (21)$$

Similarly, Eqs. (19) and (20) are unified as follows:

$$l_1m_1\varepsilon_1\omega^2e^{j\theta_1}+(l-l_2)m_2\varepsilon_2\omega^2e^{j\theta_2}+l(B_{X1}+jB_{Y1})-l_1m_1ge^{-j\omega t}-(l-l_2)m_2ge^{-j\omega t}=0 \quad (22)$$

By using the complex forces of Eqs (10) and (11) and introducing the correction quantities in terms of complex variables, as below:

$$\overline{P}_1=m_1\varepsilon_1e^{j\theta_1} \quad (23)$$

$$\overline{P}_2=m_2\varepsilon_2e^{j\theta_2} \quad (24)$$

the Eqs. (21) and (22) become

$$\overline{P}_1+\overline{P}_2=-\frac{1}{\omega^2}(\overline{A}_1+\overline{B}_1)+\frac{m_1+m_2}{\omega^2}ge^{-j\omega t} \quad (25)$$

$$l_1\overline{P}_1+(l-l_2)\overline{P}_2=-\frac{1}{\omega^2}B_1+\frac{m_1l_1+m_2(l-l_2)}{\omega^2}ge^{-j\omega t} \quad (26)$$

Solving for $\overline{P}_1$ and $\overline{P}_2$, we have

$$\overline{P}_1=\frac{\overline{B}_1l_2-\overline{A}_1(l-l_2)}{(l-l_1-l_2)\omega^2}+\frac{m_1}{\omega^2}ge^{-j\omega t} \quad (27)$$

$$\overline{P}_2=\frac{\overline{A}_1l_1-\overline{B}_1(l-l_1)}{(l-l_1-l_2)\omega^2}+\frac{m_2}{\omega^2}ge^{-j\omega t} \quad (28)$$

Since each bearing force on the rotating coordinates includes time-independent, constant and time-dependent terms synchronous to the rotating speed as illustrated in Eqs. (15) and (16), the bearing forces can be expressed in general as follows:

$$\overline{A}_1=A_{X1}+jA_{Y1}=A_{X0}+A_{XC}\cos(\omega t+\phi_{AX})+j\{A_{Y0}+A_{YC}\cos(\omega t+\phi_{AY})\} \quad (29)$$

$$\overline{B}_1=B_{X1}+jB_{Y1}=B_{X0}+B_{XC}\cos(\omega t+\phi_{BX})+j\{B_{Y0}+B_{YC}\cos(\omega t+\phi_{BY})\} \quad (30)$$

where A_{X0}, A_{Y0}, B_{X0} and B_{Y0} indicate the constant terms, and A_{XC}, A_{YC}, B_{XC} and B_{YC} and ϕ_{AX}, ϕ_{AY}, ϕ_{BX} and ϕ_{BY} indicate the magnitudes and the phases, respectively, of the time-dependent sinusoidal terms.

By introducing Eqs. (29) and (30) into Eqs. (27) and (28), we have

$$\overline{P}_1=\frac{1}{(l-l_1-l_2)\omega^2}[l_2\{B_{X0}+jB_{Y0}+f_B(\omega t)\}-(l-l_2)\{A_{X0}+jA_{Y0}+f_A(\omega t)\}+m_1(l-l_1-l_2)ge^{-j\omega t}] \quad (31)$$

$$\overline{P}_2=\frac{1}{(l-l_1-l_2)\omega^2}[l_1\{A_{X0}+jA_{Y0}+f_A(\omega t)\}-(l-l_1)\{B_{X0}+jB_{Y0}+f_B(\omega t)\}+m_2(l-l_1-l_2)ge^{-j\omega t}] \quad (32)$$

where f_A and f_B stand for the time-dependent terms, which are related to the time-varying forces due to the gravity. Since the left-hand side of Eqs. (31) and (32) are independent of time, all the time-dependent terms in the right-hand side of Eqs. (31) and (32) must vanish. Therefore, $\overline{P}_1$ and $\overline{P}_1$ in Eqs. (31) and (32) can be rewritten as follows:

$$\overline{P}_1=m_1\varepsilon_1e^{j\theta_1}=\frac{l_2B_{X0}-(l-l_2)A_{X0}+j\{l_2B_{Y0}-(l-l_2)A_{Y0}\}}{(l-l_1-l_2)\omega^2} \quad (33)$$

$$\overline{P}_2=m_2\varepsilon_2e^{j\theta_2}=\frac{l_1A_{X0}-(l-l_1)B_{X0}+j\{l_1A_{Y0}-(l-l_1)B_{Y0}\}}{(l-l_1-l_2)\omega^2} \quad (34)$$

Thus, the correction quantities $m_1\varepsilon_1$, $m_2\varepsilon_2$, θ_1 and θ_2 are obtained from Eqs. (33) and (34), as below:

$$m_1\varepsilon_1=\frac{\sqrt{\{l_2B_{X0}-(l-l_2)A_{X0}\}^2+\{l_2B_{Y0}-(l-l_2)A_{Y0}\}^2}}{(l-l_1-l_2)\omega^2} \quad (35)$$

$$\theta_1=\tan^{-1}\frac{l_2B_{Y0}-(l-l_2)A_{Y0}}{l_2B_{X0}-(l-l_2)A_{X0}} \tag{36}$$

$$m_2\varepsilon_2=\frac{\sqrt{\{l_1A_{X0}-(l-l_1)B_{X0}\}^2+\{l_1A_{Y0}-(l-l_1)B_{Y0}\}^2}}{(l-l_1-l_2)\omega^2} \tag{37}$$

$$\theta_2=\tan^{-1}\frac{l_1A_{Y0}-(l-l_1)B_{Y0}}{l_1A_{X0}-(l-l_1)B_{X0}} \tag{38}$$

4. Measurement Outline and Simulation

4.1 Forces in the stationary frame

Equations (35) to (38) outlined in the previous section indicate that the correction quantities $m_2\varepsilon_2$, θ_1 and θ_2 are expressed in terms of the bearing forces A_{X0}, A_{Y0}, B_{X0} and B_{Y0}. Although these forces can be found experimentally, the method of measurement is not straightforward in the sense that they are not isolated quantities but are amalgamated with certain components. A brief description of the method of extraction is illustrated below.

Transforming the force vector $\overline{A}_1$ into the stationary coordinates yields

$$\overline{A}=\overline{A}_1e^{j\omega t}=(A_{X_1}+jA_{Y_1})e^{j\omega t}$$

By replacing the time-independent terms in Eq. (15) by $A_{X0}+jA_{Y0}$ of Eq. (29), and then substituting the results into the above equation, we have

$$\overline{A}=\frac{mgl_B}{l_A+l_B}+A_{X0}\cos\omega t-A_{Y0}\sin\omega t+j(A_{Y0}\cos\omega t+A_{X0}\sin\omega t) \tag{39}$$

Similarly, we have:

$$\overline{B}=(B_{X_1}+jB_{Y_1})e^{j\omega t}=\frac{mgl_A}{l_A+l_B}+B_{X0}\cos\omega t-B_{Y0}\sin\omega t+j(B_{Y0}\cos\omega t+B_{X0}\sin\omega t) \tag{40}$$

By rearranging Eqs. (39) and (40), we have

$$\overline{A}=\frac{mgl_B}{l_A+l_B}+\sqrt{A_{X0}{}^2+A_{Y0}{}^2}e^{j(\omega t+\phi_A)} \tag{41}$$

$$\overline{B}=\frac{mgl_A}{l_A+l_B}+\sqrt{B_{X0}{}^2+B_{Y0}{}^2}e^{j(\omega t+\phi_B)} \tag{42}$$

where

$$\phi_A=\tan^{-1}\frac{A_{Y0}}{A_{X0}} \tag{43}$$

$$\phi_B=\tan^{-1}\frac{B_{Y0}}{B_{X0}} \tag{44}$$

4.2 Calculation of A_{X0}, A_{Y0}, B_{X0} and B_{Y0}, from measurements

In the experiments, only one axis between the X and Y axes at each bearing can be chosen for measurement since the same information is produced from both the X and Y axes measurements, as illustrated in Figs. 3 and 4.

At bearing A, by letting the measured amplitude be $(Amp_{A\text{-}meas})$ and the measured phase of Fig. 3 be $(\phi_{A,meas})$, which is governed by the reference (or trigger) position on the periphery of

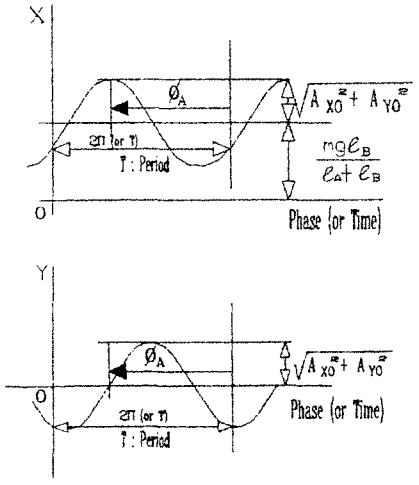

Fig. 3 X and Y components of force on bearing A.

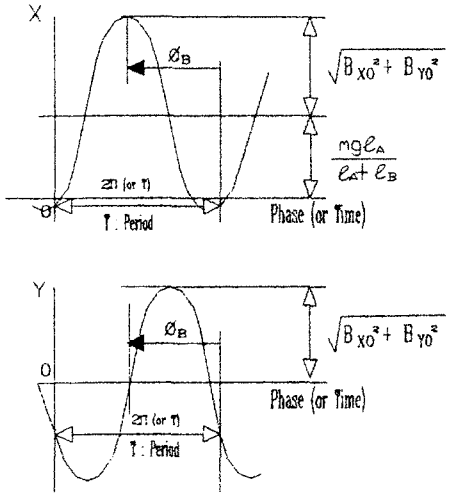

Fig. 4 X and Y components of force on bearing B.

rotor, it is possible to obtain the following relations:

$$A_{X0}^2+A_{Y0}^2=(Amp_{A,meas})^2$$
$$\frac{A_{Y0}}{A_{X0}}=\tan(\phi_{A,meas})$$

Consequently, A_{X0} and A_{Y0} are derived as

$$A_{X0}=\begin{cases}\dfrac{(Amp_{A,meas})}{\sqrt{1+\tan^2(\phi_{A,meas})}} & \text{for } 0\le(\phi_{A,meas})\le\dfrac{\pi}{2},\\ & \dfrac{3\pi}{2}\le(\phi_{A,meas})\le 2\pi\\ \dfrac{-(Amp_{A,meas})}{\sqrt{1+\tan^2(\phi_{A,meas})}} & \text{for } \dfrac{\pi}{2}\le(\phi_{A,meas})\le\dfrac{3\pi}{2}\end{cases} \tag{45}$$

$$A_{Y0}=\begin{cases}\dfrac{(Amp_{A,meas})\tan(\phi_{A,meas})}{\sqrt{1+\tan^2(\phi_{A,meas})}} & \text{for } 0\le(\phi_{A,meas})\le\pi\\ \dfrac{-(Amp_{A,meas})\tan(\phi_{A,meas})}{\sqrt{1+\tan^2(\phi_{A,meas})}} & \text{for } \pi\le(\phi_{A,meas})\le 2\pi\end{cases} \tag{46}$$

Similarly, B_{X0} and B_{Y0} for bearing B are expressed as

$$B_{X0}=\begin{cases}\dfrac{(Amp_{B,meas})}{\sqrt{1+\tan^2(\phi_{B,meas})}} & \text{for } 0\le(\phi_{B,meas})\le\dfrac{\pi}{2},\\ & \dfrac{3\pi}{2}\le(\phi_{B,meas})\le 2\pi\\ \dfrac{-(Amp_{B,meas})}{\sqrt{1+\tan^2(\phi_{B,meas})}} & \text{for } \dfrac{\pi}{2}\le(\phi_{B,meas})\le\dfrac{3\pi}{2}\end{cases} \tag{47}$$

$$B_{Y0}=\begin{cases}\dfrac{(Amp_{B,meas})\tan(\phi_{B,meas})}{\sqrt{1+\tan^2(\phi_{B,meas})}} & \text{for } 0\le(\phi_{B,meas})\le\pi\\ \dfrac{-(Amp_{B,meas})\tan(\phi_{B,meas})}{\sqrt{1+\tan^2(\phi_{B,meas})}} & \text{for } \pi\le(\phi_{B,meas})\le 2\pi\end{cases} \tag{48}$$

Equations (45) to (48) present the coveted terms A_{X0}, A_{Y0}, B_{X0} and B_{Y0} in terms of the measured quantities $(Amp_{A,meas})$, $(Amp_{B,meas})$, $(\phi_{A,meas})$ and $(\phi_{B,meas})$. Therefore, substituting the results (45) to (48) into Eqs. (35) to (38) yields the correction quantities and their locations: namely, $m_1\varepsilon_1$, $m_2\varepsilon_2$, θ_1 and θ_2.

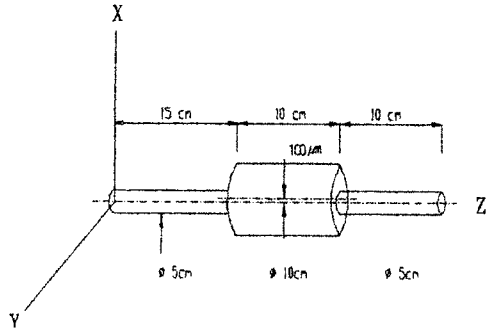

Fig. 5 Simulation model.

4.3 Simulation

An example model of Fig. 5 is considered to show the validity of the method. The model is composed of three elements: the first element of 15 cm length and 5 cm diameter, the second element of 10 cm length and 10 cm diameter and the third element of 10 cm length and 5 cm diameter. The density of rotor material is 7. 8. The constant rotational speed is $\omega=1000 rad/s$. The second element is $100\mu m$ offset from the rotation axis, and the angle θ in Fig. 1 which indicates the unbalance direction is assumed to be zero for simplicity. The two balancing planes are positioned at Z=15 cm and 25 cm respectively.

The coordinates of the mass center G of the entire rotor system are (6.15385×10^{-3}, 0, 18.6538) in cm unit. Using the parallel-axis theorem and noting that the product of inertia of each rod is zero with respect to centroidal axes, we have:

$$I_{xz}=0.082469\text{kg}\cdot\text{cm}^2$$
$$I_{yz}=0$$

with respect to G. Calculating the bearing reaction forces using Eqs. (15) and (16) and transfor-

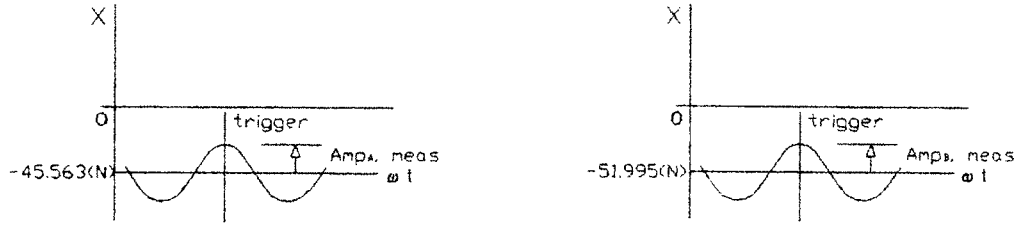

(a) Bearing A (b) Bearing B

Fig. 6 Bearing forces on the vertical(X-) axis.

ming them into the stationary coordinates, the forces applied to the bearings on the vertical axes (X-axes) can be plotted as in Fig. 6. In the figure, Amp_{Ameas} is 262.547(N) and $Amp_{B,meas}$ is 350.062(N).

In this simulation the trigger(reference) signal is tuned to coincide with the unbalance direction for simplicity. Since the trigger position coincides with the peak level in forces, we have

$$\phi_{A,meas}=0$$
$$\phi_{B,meas}=0$$

Using Eqs. (45) to (48), we have

$$A_{X0}=262.547(N)$$
$$A_{Y0}=0$$
$$B_{X0}=350.062(N)$$
$$B_{Y0}=0$$

Introducing these values into Eqs. (35) to (38) yields the correction quantities as follows:

$$m_1\varepsilon_1=3.06305\times10^{-4}\text{kg}\cdot m$$
$$\theta_1=\tan^{-1}\left(\frac{0}{(0.1)(350.062)-(0.25)(262.547)}\right)$$
$$=180°$$
$$m_2\varepsilon_2=3.06305\times10^{-4}\text{kg}\cdot m$$
$$\theta_2=\tan^{-1}\left(\frac{0}{(0.15)(262.547)-(0.2)(350.062)}\right)$$
$$=180°$$

The simulation results are acceptable within common engineering practice. The total correction quantity $6.12610\times10^{-4}\text{kg}\cdot m$ is balanced with the unbalance on the second element. Two correction quantities on the balancing planes at Z =15cm and 25cm eliminate the dynamic unbalance also.

5. Conclusion

In this study, the correction masses on the two arbitrary planes along a rigid-rotor shaft are derived from the basic concept of three-dimensional rigid body dynamics. The correction quantities on two arbitrary balancing planes are analytically found in terms of the bearing force measurements.

In measurements, this method uses one measuring point (or sensor) at each bearing. If suitable equipments for driving the rotor and sensing the bearing forces are supported technically, this study provides simple, time-saving and useful tool, because the method requires only the bearing force measurements from a single run and simple information: the distance between two bearings and the positions of balancing planes from the bearings. Using a simulation example, the correction quantities calculated from the measurement are shown to compensate the unbalance due to rotor skewness.

Acknowledgement

This work was supported by Jeonju University Research Program 1996.

Reference

Darlow, M. S., 1987, "Balancing of High-Speed Machinery: Theory, Methods and Experimental Results," *Mechanical Systems Signal Processing*, Vol. 1, No. 1, pp. 105~134.

Darlow, M. S., 1989, *Balancing of high-speed machinery*, Chapter 4, Spring-Verlag, New York.

Everett, L. J., 1987, "Two-Plane Balancing of a Rotor System Without Phase Response Measurements," *ASME J. Vibration, Acoustics, Stress, Reliability in Design*, 109, pp. 162~167.

Hard Bearing Balancing Machines Catalogue, Carl Schenck.

ISO 1925, 1981, "Balancing-Vocabulary," International Organization for Standardization.

Kwon Y. -S., et al., 1995, "Development of a Hard Bearing Type Balancing Machine," *Spring Conference Proc., J. Korean Society of Precision Engineering*, pp. 773~777.